

# Modeling and Validation of the Ice Growth in an Ice Storage System

Stefanie Paulini<sup>1</sup>, Tobias Plessing<sup>1</sup> and Dieter Brüggemann<sup>2</sup>

*1. Institute for Water and Energy Management at Hof University, Hof 95028, Germany*

*2. Department of Engineering Thermodynamics and Transport Processes (LTTT), University of Bayreuth, Bayreuth 95447, Germany*

**Abstract:** This work deals with the optimization of the icing process in an ice storage system. It is focused on the improvement of the icing behavior, which is to be achieved by different heat exchanger geometries in the ice storage tank. Therefore, CFD simulations were implemented to acquire and visualize the flow conditions, the temperature behavior and the growth of the ice layer during the cooling process. The results are compared and validated with model experiments on an experimental ice storage. It could be shown that the heat extraction of current technologies can be increased by more than 50% by using geometries that are more efficient.

**Key words:** CFD simulation, ice storage, model validation.

## 1. Introduction

To decrease the use of fossil fuels and greenhouse gas emissions for the provision of heating in buildings, heat pumps combined with clean electricity are a preferable option and are gaining importance worldwide. Heat pumps can be used with different heat sources like air, ground or solar. As air source heat pumps are cheap and easy to install, they are a preferred system in Germany although the efficiency is limited especially during the cold season. Ice storage systems enable to supply ground source heat pumps with temperatures above  $-10\text{ }^{\circ}\text{C}$  for a longer time. To increase the annual operating efficiency and the overall efficiency of the heat pump system, the ice storage has to be fully exploited. Therefore, the flow conditions in the ice storage tank have to be analyzed. A homogeneous mixing during the icing process enables a longer sensible heat extraction and temperatures above  $0\text{ }^{\circ}\text{C}$  for a longer time. In addition, the  $4\text{ }^{\circ}\text{C}$  sump could be avoided by homogeneous mixing.

In the presented project, the heat input into a solar ice storage with a helix and a star-shaped heat exchanger is examined. In addition to model experiments, CFD simulation is used for the acquisition and visualization of the flow conditions, the temperature profile and the ice build-up. The aim is to optimize the heat input into the ice storage tank and the icing process upon the heat exchanger plates by adapting the heat exchanger geometry.

## 2. Boundary Conditions

The main aim is to enhance the overall icing process in the ice storage tank. The convective flow within the water tank should be improved in order to achieve a more homogeneous mixing in the ice storage system. The aim of the further investigation is to optimize the ice building process in the ice storage tank along the heat exchanger surface. By keeping the ice built up parallel to the heat exchanger plates as long as possible, the temperature of the return flow of the heat pump decreases slowly and the heat pump can be supplied with temperatures above  $-10\text{ }^{\circ}\text{C}$  for a longer period. This increases the annual operating efficiency and thus the overall efficiency of the heat

---

**Corresponding author:** Stefanie Paulini, M.Sc., research field: energy science.

pump system. An adapted ice growth on the heat exchanger plates increases the proportion of the water volume which could be iced. The investigations of Carbonell et al. [1] showed that plates made of polypropylene have a lower overall heat transfer coefficient during sensible cooling and solidification than flat plates made of stainless steel. The experiments also showed that these polypropylene plates have a stable overall heat transfer coefficient during the sensible cooling and the solidification. Considering that the ice storage should be used for long term issues, a stable heat transfer coefficient supports a constant long time heat extraction from the ice storage. The influence of the heat exchanger geometry on the flow, the temperature layering and the ice growth is pictured and analyzed by CFD simulations. Therefore, 2D and 3D models of the ice storage and heat exchangers are built with ANSYS Fluent. The simulation models are validated by model experiments on a horizontally divided hemispherical experimental ice storage on a scale of 1:2 to the original ice storage. Numerical simulation of the phase change is tried to be solved by several methods. Some of them are compared in the study of König-Haagen et al. [2]. This study shows that though using small simulation areas, errors between the numerical results and reference solutions could be detected. In the following work, the simulation is done for the whole ice storage tank, so errors between the simulation results and the measurements were predicted and could not be prevented.

### 3. Setup and Results

Based on former CFD simulations, a model test bench was created for the visualization of the icing process in the ice storage tank. The test bench consists of an 8 kW heat pump with a refrigerating capacity of 6 kW, a 2.5 m<sup>3</sup> horizontally divided hemispherical ice storage tank and small storage with electrical heating rod as shown in Fig. 1.

The ice storage tank was isolated to reduce the heat

input from the surrounding area. The small storage with the heating rod was installed to reheat the ice storage after the icing experiments. The water-filled tanks on the ice storage counteract the rising buoyancy force of the ice during the icing process. As a basis for the first model experiments, a helix heat exchanger was chosen. The ice storage was iced until the return flow temperature of the heat pump reached the switch-off temperature of -10°C. Afterwards the heat exchanger was replaced by a star-shaped geometry with an arrangement of 24 heat exchanger plates. Thereafter, the number of the heat exchanger plates was halved from 24 to 12 plates to improve the icing process. Six temperature sensors in the ice storage and one temperature sensor in each case in the flow and return flow of the primary circuit of the heat pump documented the icing process.

The simulation of the phase change was realized by the ANSYS Fluent solidification and melting tool. The solver settings were designed according to Al-abidi et al. [3] and Nayak et al. [4]. To solve the simulation the pressure-based Navier-Stokes solution algorithm with the absolute velocity formulation was used. The time option was set transient to enable a time-dependent solution.

The geometry was transferred to a 1:1 scale CFD model, simulated with boundary conditions of the model experiments and then validated with the data from the model experiments.

The helix heat exchanger was realized with 2D-CFD simulation. The model was simulated in horizontal and vertical cut through the heat exchanger and the ice storage as seen in Fig. 2.

The points of temperature measurement were set to the same places as the temperature sensors in the model test bench. Five sensors were set in a horizontal row to picture the temperature behavior through the horizontal cut of the ice storage and one was set to the ground of the ice storage to picture the 4°C sink at the bottom of the tank. This sink is due to the anomaly of water.



Fig. 1 Test bench with isolated ice storage (left), storage with heating rod (middle) and heat pump (right).

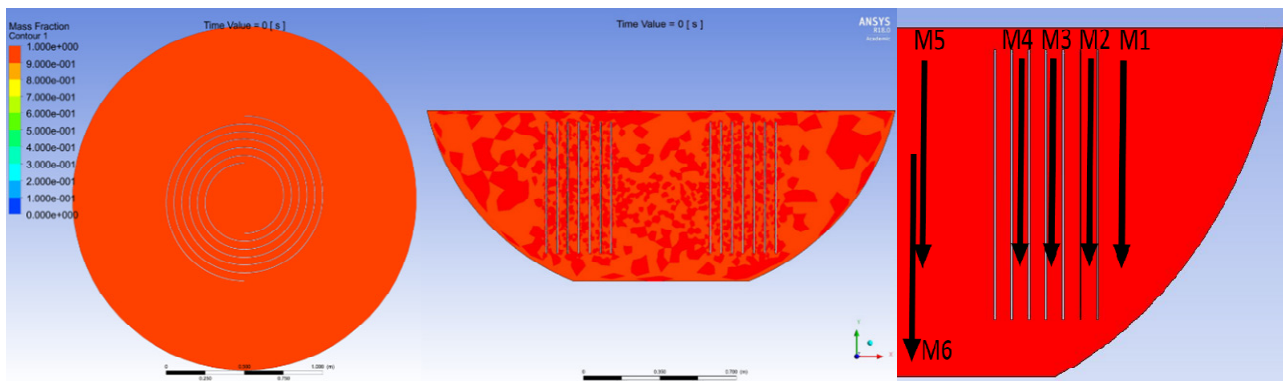


Fig. 2 Horizontal (left) and vertical (middle) cut through the helix heat exchanger and ice storage with points of temperature measurement (right).

The heat exchanger temperature from the model experiments was implemented as a boundary condition for the plate temperature for the simulations. The simulation models were validated and adjusted with the measurement results from the model experiments with the helix heat exchanger.

The star shaped heat exchanger was simulated with 3D-CFD simulation. Due to the radial symmetry of the model, only 1/12 of the ice storage was transferred to a simulation model. The modelled geometry with two heat exchanger plates is shown in Fig. 3.

The red crosses represent the six points at which the temperature is logged during the simulations. They are similar with the six temperature sensors in the ice storage volume at which the temperature is measured during the experiments at the model test bench. Similar to the 2D-CFD simulation the heat exchanger

temperature from the model experiments was implemented as a boundary condition for the plate temperature for the simulations. The simulation models were also validated and adjusted with the measurement results from the model experiments with the star-shaped heat exchanger.

The results of the 2D-CFD simulation of the helix heat exchanger and the measurements at the test bench are shown below. The simulation showed good accordance with the results of the model experiments from the test bench. The temperature profile of the temperature sensor 2 until the switch-off point of the heat pump is pictured in Fig. 4.

The latent heat transfer could be mapped very well in the simulation (blue line) by the long temperature stability during the ice build-up between 1:30 and 6:00 of the simulation time. The measured temperature

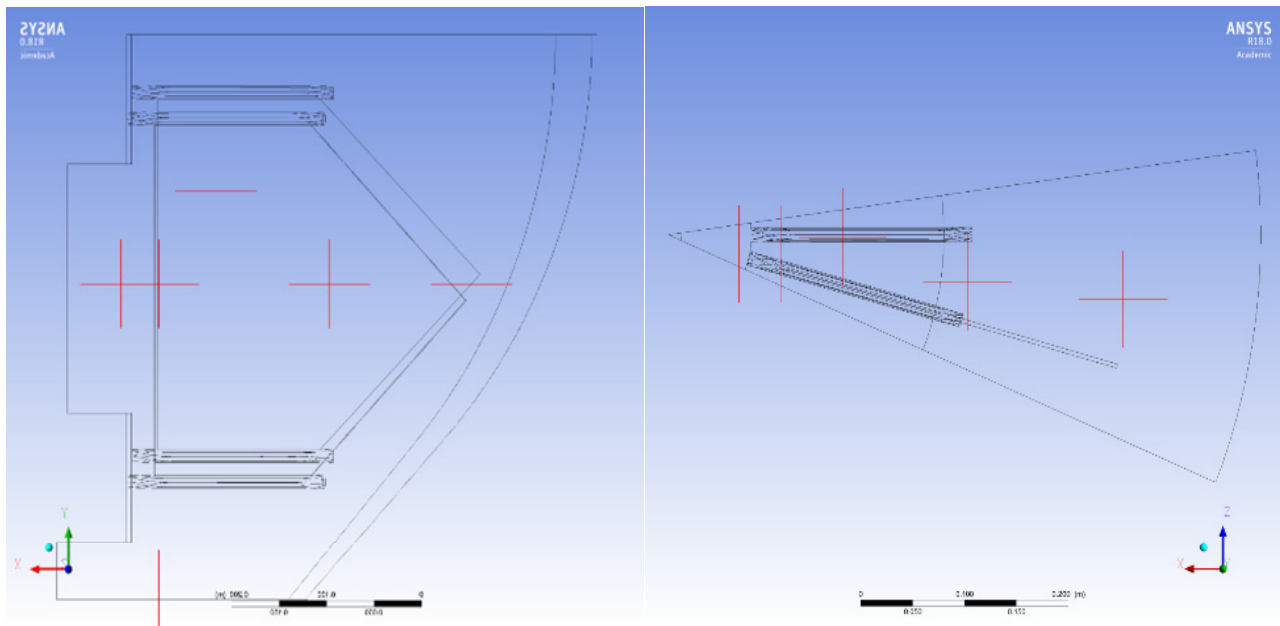


Fig. 3 Arrangement of the temperature sensors in the simulated part with two heat exchanger plates.

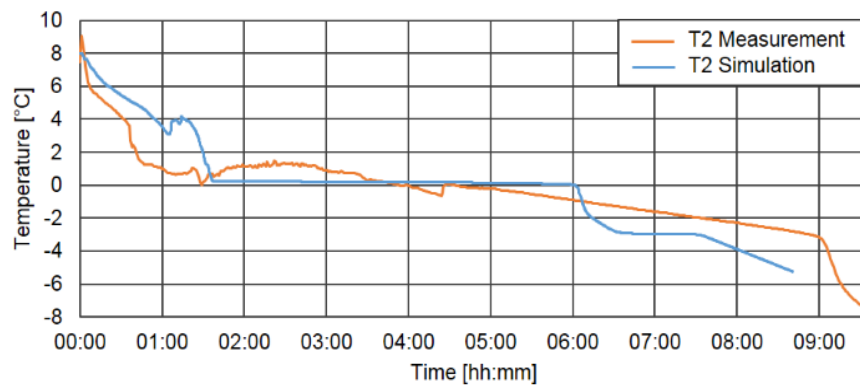


Fig. 4 Temperature profile of the model experiment (orange) and the simulation (blue) during the icing process.

(orange line) shows, that some effects like supercooling could only be described inadequately by the simulation. Nevertheless, the overall temperature behavior of the simulations fits with the experimental values. The decreasing temperature line of the model experiment (orange line) pictures the dipping of the temperature sensor into the ice. The temperature drop at the end of the time line describes the point at which the ice walls grow together.

Several model experiments on the helix heat exchanger showed the reproducibility of the individual temperature behavior. Slight divergences could be explained by the different starting temperatures in the ice storage volume. The simulation clearly shows the

temperature stratification in the ice storage with the 4 °C sink at the bottom of the ice storage tank. Although the heat exchanger plates are already freezing, half of the fluid volume is still warmer than 1 °C. These two circumstances lead to the fact that the heat exchanger plates begin to freeze in the upper third and the lower parts of the plates are not yet frozen at the end of the simulation. Though the phenomena of starting freezing in the upper third of the heat exchanger plates are also pictured in the model experiments, it is shown in Fig. 5.

This also shows the unfavorable shape of the heat exchanger compared to the surrounding fluid in the simulation. Due to the geometry, only a fraction of the

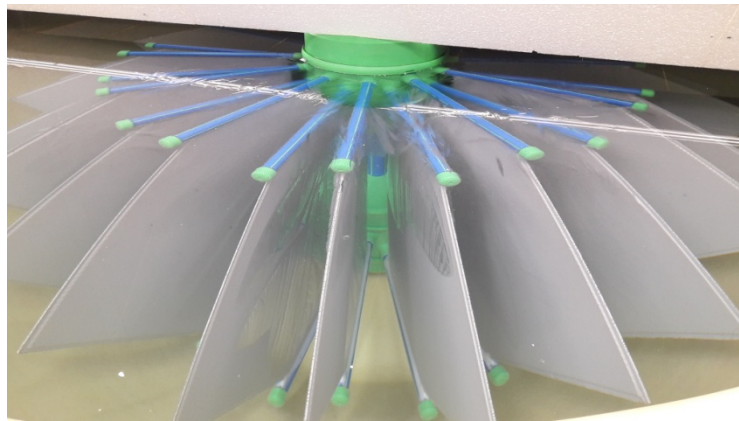


**Fig. 5** Beginning of freezing at the star-shaped heat exchanger with 24 plates.

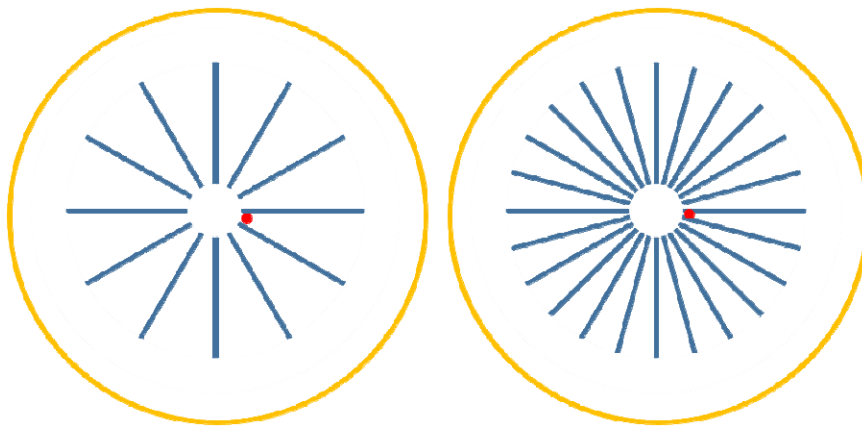


**Fig. 6** Arrangement of the heat exchanger plates and temperature sensor 1 in the star-shaped model with 12 plates (left) and 24 plates (right).

existing fluid can really be iced. This results in a latent heat extraction of 50.59 kWh in 8 h and 42 min by a heat exchanger surface of 34 m<sup>2</sup>.

Based on these basic experiments and simulations, a preferred geometry is to be determined, which represents the basis for a subsequent development. A star shaped heat exchanger with 24 plates was chosen for the further analyses. The geometry was reduced to 12 plates after the first experiments. The number of heat exchanger plates influences the point on which the ice walls on the plates grow together and the temperature in the return flow of the heat pump drops off. The arrangement of the star-shaped heat exchanger with 12 and 24 plates with the temperature sensor 1 (red dot) is shown in Fig. 6.

The temperature sensor 1 is the point, where the ice grows together first. When the temperature at sensor 1

falls below 0 °C, it is dipping into the ice. Due to the reduction of heat exchanger plates, the specific extraction of heat of each heat exchanger plate is doubled compared to the star-shaped heat exchanger with 24 plates.

The results of the star-shaped heat exchanger are shown below. The star shaped heat exchanger with 24 plates has a theoretical ice thickness of 13.3 cm. During the icing experiments at the ice storage test bench, this value could not be reached. One of the reasons was the small distance between the backs of the plates in the middle of the star geometry. That led to a fast growing together of the ice walls, which reduced the overall ice surface. Therefore, the temperature at the heat pump return flow decreased and the heat pump stopped working. The ice buildup after one icing cycle until the heat pump shut-off at -10 °C is pictured in Fig. 7.



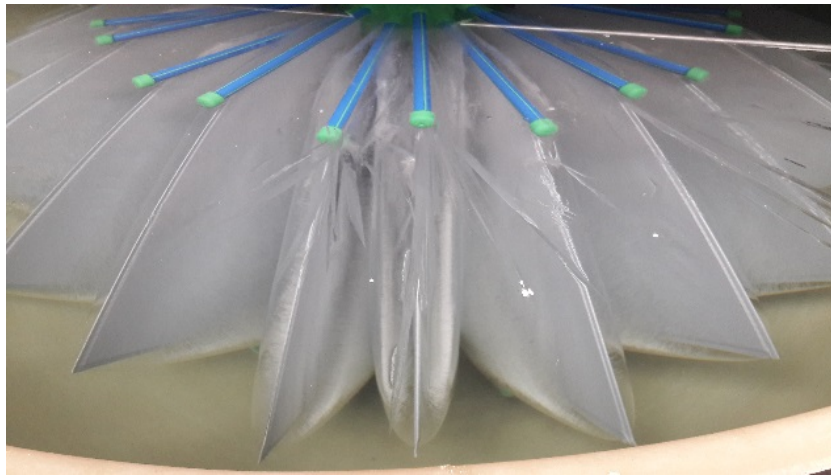


**Fig. 6** Ice built-up after one icing cycle of the heat pump at the star shaped heat exchanger with 24 plates.

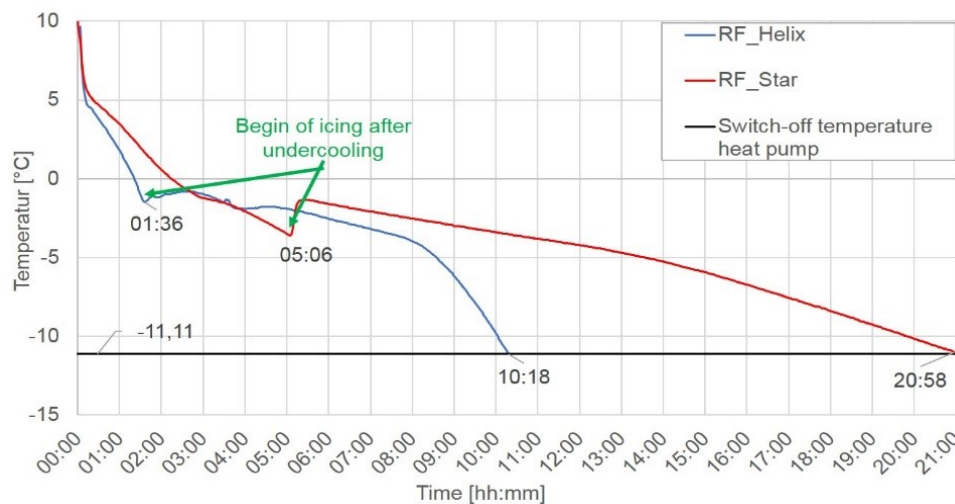


**Fig. 7** Difference of the return flow temperatures of the primary circuit of the heat pump with helix (blue) and star-shaped (red) heat exchanger with 24 plates.

The picture shows the small ice layer of only about 6 cm. The back surfaces of the plates are grown together, which can also be seen in the temperature profile of the temperature sensor 1 and the return flow temperature of the primary circuit of the heat pump. The ice built-up results in a latent heat extraction of 105.14 kWh in 15 h 52 min by a heat exchanger surface of 34 m<sup>2</sup>, which is double the value of the helix heat exchanger. The comparison of the return flow temperatures of the primary circuit of the heat pump of the helix heat exchanger and the star shaped with 24 plates is illustrated in Fig. 8.

The improved flow through the ice storage with star-shaped heat exchanger significantly delayed the

onset of icing and increased the amount of sensible heat extracted by 50%. The rapid decreasing in the return flow temperature of the helix structure after 8 hours of experimentation is attributable to the coalescing ice layers between the helical turns and thus to a rapid reduction of the heat transfer surface. In the star-shaped geometry, the heat transfer surface is reduced only slowly, which is reflected in the gradually decreasing temperature curve of the return flow temperature. In both cases, it comes to a significant supercooling of the heat transfer medium before the icing of the heat exchanger surfaces starts. In the helical geometry, the supercooling is -1.8°C, in the star-shaped structure even -3.7°C. Since the sensitive heat depends on the



**Fig. 8** Thickness of the ice walls of 14 cm from ice surface to ice surface with plate in the middle after one icing circuit with the star-shaped heat exchanger with 12 plates.

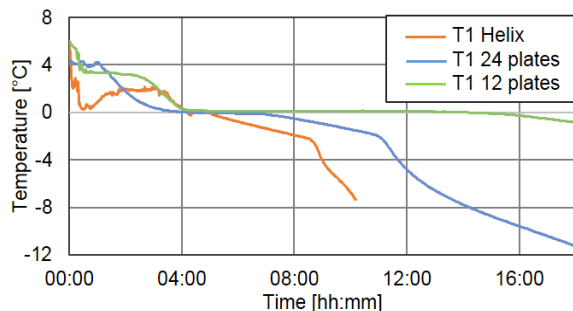


**Fig. 9** Difference of the temperature profile of temperature sensor 1 with helical heat exchanger (orange), 24 plates (blue) and 12 plates (green) heat exchanger during the icing process.

flow, the amount of water and the start temperature of the water volume in the ice storage tank, it is not considered in this work.

The icing experiments with the star-shaped heat exchanger with 12 plates showed good accordance to the theoretical icing behavior. The theoretical calculated ice thickness of 6.6 cm per plate surface could be reached during the icing process as pictured in Fig. 9.

Due to the big distance between the individual plates, the ice built-up could proceed parallel during the whole icing process. This shows that the reducing heat exchanger surface was the limiting factor for the ice built-up with 24 plates and helix heat exchanger in

the former experiments. This restriction could also be outlined by the temperature profiles of temperature sensor 1 during the icing experiments with the helix heat exchanger and the star-shaped heat exchanger with 24 and with 12 plates in Fig. 10.

The drop off in the orange and blue temperature profile of the helical and the 24 plates heat exchanger is owed to the coalescing ice layers and the rapid reduction of the heat transfer surface. The heat exchanger with 12 plates starts icing together at the end of the icing experiments. This shows, that there is a parallel icing during the whole process.

The difference of the icing behavior of the heat exchanger with 24 and with 12 plates is clearly shown in Fig. 11. It illustrates the difference in the return flow temperatures of the primary circuit of the heat pump for 12 and 24 plates of the star-shaped heat exchanger and the temperature sensor 1 in both cases on the model test bench.

The plate temperature (12 plates) clarifies the beginning of the icing process after the undercooling process.

The time of the parallel icing from the beginning of icing after undercooling until the temperature drop-off is much longer at the heat exchanger with 12 plates than with 24 plates. The undercooling of the return flow temperature with 24 plates is  $-2.5^{\circ}\text{C}$ , while the undercooling of the return flow temperature with 12 plates reaches  $-4.8^{\circ}\text{C}$ . One of the reasons for this effect is the improved flow conditions at the geometry with 12 plates.

Though the 3D simulation of the star-shaped heat exchanger with 24 plates took several months to calculate, it is only considered for a qualitative statement. The ice built-up of the 3D simulation and the icing experiment with the star-shaped heat exchanger with 24 plates is shown in Fig. 12.

Due to the coarse grid, the surface of the simulated ice layer is irregular. The simulation resulted in an ice volume of  $0.616\text{ m}^3$  or  $576\text{ kg}$ , while the experiment resulted in a calculated ice layer of about  $590\text{ kg}$ .

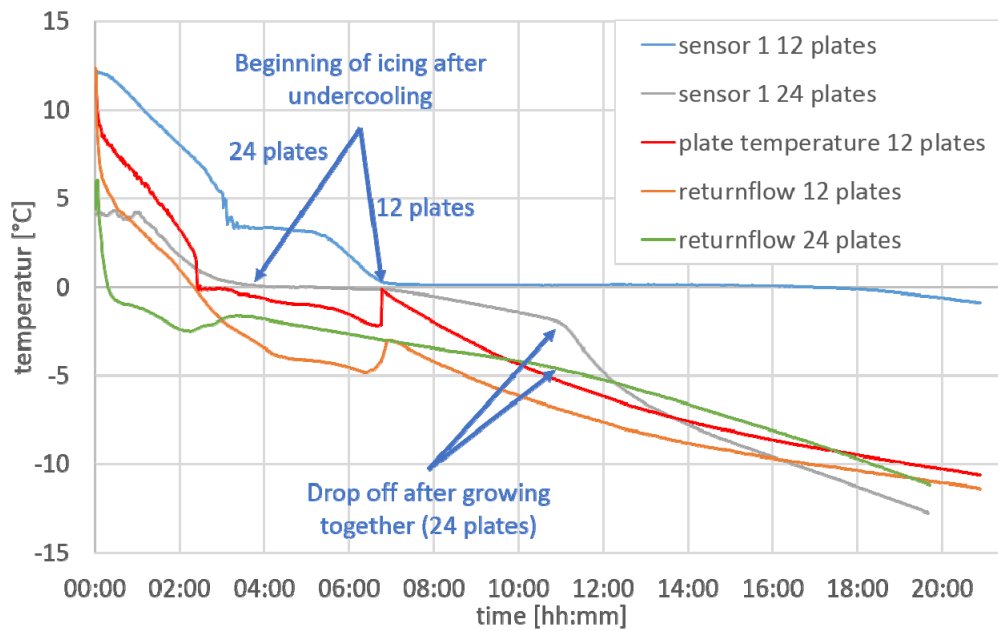


Fig. 10 Difference of the return flow temperatures of the primary circuit of the heat pump with 12 (yellow) and 24 (green) heat exchanger and of the temperatures between the plates (blue and grey).

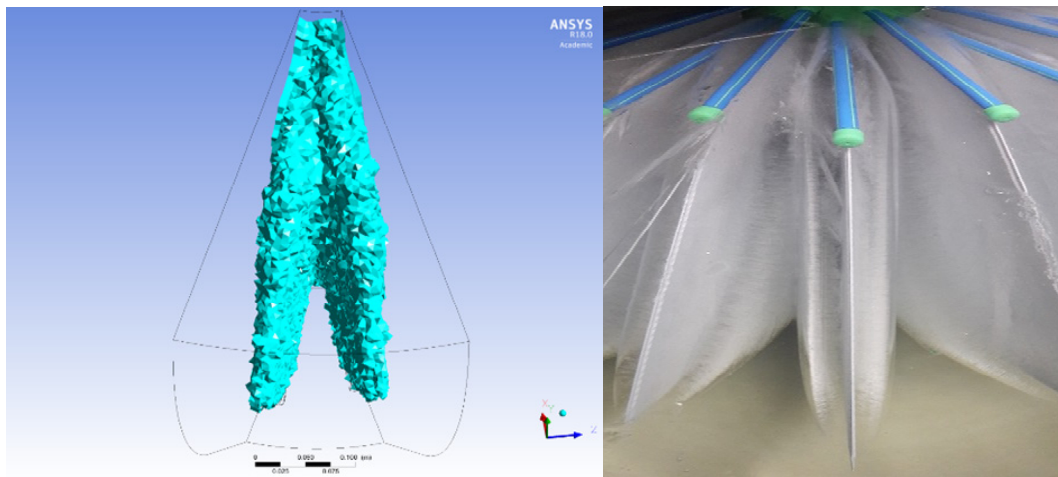


Fig. 11 Ice built-up in the simulation (left) and icing experiment (right) for the star-shaped heat exchanger with 24 plates.

#### 4. Conclusion and Future Work

The modeling of an ice storage system with 2D- and 3D-CFD simulation with ANSYS Fluent and the validation of these simulations with model test bench experiments is shown in this work. The temperature behavior during the cooling and icing process in the ice storage could be mapped very well despite a time gap by 2D-CFD simulations. The ice build-up could be predicted well by the 2D- and 3D-CFD simulations. The simulations and the experiments showed the

increasing of the heat extraction by using a star-shaped heat exchanger geometry.

The accuracy of the 2D simulations should be further improved by adapting the parameters and boundary conditions. The 3D simulation should be improved by model reduction.

#### Acknowledgements

This work has been funded by the Bavarian State Ministry of Education, Science and the Arts within the framework “Technologie Allianz Oberfranken (TAO)”



and the Federal Ministry for Economic Affairs and Energy within the framework “Zentrales Innovationsprogramm Mittelstand (ZIM)”. The authors gratefully acknowledge this support.

## References

- [1] Carbonell, D., Granzotto, M., Battaglia, M., Philippen, D., and Haller, M. Y. 2016. “Experimental Investigations of Heat Exchangers in Ice Storages for Combined Solar and Heat Pump Systems.” In *Proceedings of the 11th International Conference on Solar Energy for buildings and Industry*, Eurosun.
- [2] König-Haagen, A., Franquet, E., Pernot, E., and Brüggemann, D. 2017. “A Comprehensive Benchmark of Fixed-Grid Methods for the Modeling of Melting.” *International Journal of Thermal Sciences* 118: 69-103.
- [3] Al-abidi, A. A., et al. 2013. “CFD Applications for Latent Heat Thermal Energy Storage: A Review.” *Renewable and Sustainable Energy Reviews* 20: 353-63.
- [4] Nayak, A. O., Ramkumar, G., Manoj, T., and Vinod, R. 2011. “Comparative Study between Experimental Analysis and CFD Software Analysis of PCM material in Thermal Energy Storage System.” *International Journal of Chemical Engineering and Applications* 2 (6): 401-7.